X-ray study of the crystallographic transformation in hydrogen below 1.5 K

J. V. Gates,* P. R. Granfors, B. A. Fraass, and R. O. Simmons
Physics Department and Materials Research Laboratory, University of Illinois at Urbana-Champaign, Urbana, Illinois 61801
(Received 28 August 1978)

The fcc to hcp and hcp to fcc phase transformations in single crystals of hydrogen have been studied using x-ray diffraction techniques. The transformation temperature T^* has been mapped as a function of orthohydrogen concentration χ in the region of $0.17 < T^* < 1.5$ K and $0.48 < \chi < 0.7$. The fcc to hcp transformation temperature extrapolates to zero near a concentration of 0.49. The transformation temperatures and widths agree with other experimental results at higher temperatures, but exclude low-concentration NMR data in the literature from being associated with the crystallographic transformation in bulk samples.

I. INTRODUCTION

The existence of different phases in solid hydrogen is well established. The transition between adjoining phases is pressure, temperature, and orthohydrogen-concentration (χ) dependent. The phases differ in rotational order and crystallographic structure. Although most of the P-χ-T phase diagram is little understood,[1] there has been considerable experimental effort devoted to understanding the zero-pressure plane. Several experimental techniques have been used to study the transition temperatures, T^*, at zero pressure as a function of orthohydrogen concentration. It was found that the transition temperature and concentration dependence of the changes in the cw NMR line shape,[2,3] λ anomalies in the specific heat,[4] changes in $(dP/dT)_V$,[5,6] and x-ray studies[7,8] closely agreed for concentrations greater than 0.67. The x-ray work identified the crystal structure to be hexagonal close packed (hcp) for temperatures greater than T^* and face-centered cubic (fcc) for temperatures less than T^*. In addition, the NMR line shape implied that the molecules were rotationally ordered for temperatures less than T^*, that is, in the fcc structure, and were rotationally disordered for temperatures greater than T^*, that is, in the hcp structure. The theoretically predicted[9,10] long-range-ordered space group $Pa3$ for the ordered state of the fcc structure has since been shown to exist for deuterium by neutron studies[11] and for hydrogen by Raman studies.[12] The crystallographic transformation shows hysteresis between the fcc to hcp and the hcp to fcc transformations, and is martensitic in nature.[11]

With the exception of the $(dP/dT)_V$ work, these aforementioned experiments were limited to concentrations greater than 0.67, for which T^* is greater than 1.0 K. The $(dP/dT)_V$ results extended the concentration dependence down to $\chi = 0.55$, for which T^* is greater than 0.5 K. Recent NMR (cw,[13,14] pulsed,[15] and[16] T_1) measurements, utilizing dilution refrigerators, have studied the transition to concentrations as low as 0.1 with a resulting T^* in the range 0.05 to 0.2 K. Although the low-temperature ($T^* < 0.5$ K) and low-concentration ($\chi < 0.55$) NMR results are not mutually consistent, it has been believed that the relationship between the structure and molecular ordering is similar to the high-temperature results. There is close agreement between x-ray and NMR changes for temperatures greater than 1.0 K and an apparent bridging of the gap in transition temperature between the lower-temperature NMR work and the higher-temperature NMR work by the $(dP/dT)_V$ results. Therefore, it has been implicitly assumed and explicitly stated that the low-concentration ordered state was also fcc. It is the purpose of the present work to test this assumption.

In the experiments presented here, the fcc to hcp and hcp to fcc transformations have been observed primarily by watching the decrease in intensity and reappearance, respectively, of the Cu $K\alpha$ {200} Bragg reflection from a single fcc hydrogen crystal. When there was no reappearance of the fcc structure, the hcp structure was verified. The intensity of the Bragg peak was monitored on a position-sensitive x-ray detector as a function of time and temperature. A dilution refrigerator was used to cool the samples to temperatures near 0.1 K.

The following notation has been adopted throughout this work: In general the transition temperatures will be represented by T^* independent of the particular experiment referenced. When it is necessary to reference a particular crystallographic transformation the notation $T^*_{\text{fcc}\rightarrow\text{hcp}}$ and $T^*_{\text{hcp}\rightarrow\text{fcc}}$ will be used. The concentration χ always refers to that of orthohydrogen.

II. EXPERIMENTAL METHOD

A. Measurement techniques and apparatus

In working with single crystals of solidified gases below one Kelvin it is more practical to move the x rays than to move the crystal for orientational purposes. For this reason a massive 40-cm radius three-circle diffractometer[17] is used to orient the x-ray tube and detector about a fixed crystal. The diffractometer can provide access to $\frac{3}{2}\pi$ sr of solid angle. In addition to this angular freedom, the diffractometer has translational x, y, and z drive capabilities with an accuracy of 0.03 mm. The linear drives not only allow for centering the diffractometer about the crystal, but also provide a means of mapping the dimensions of a single crystal and determining its quality.

Due to the relatively fast conversion of orthohydrogen to parahydrogen, there is a time constraint when attempting to observe the transformation in a narrow concentration range. This requires gathering the maximum amount of information in as short a time period as possible. For this reason a position-sensitive detector, PSD, was used. The PSD allows one to record the Bragg peak position, shape, amplitude, and integrated intensity simultaneously.

The output of the PSD and its associated electronics is fed into a 1024 channel multichannel analyzer. The accumulated data are visually displayed as the number of events (scattered photons) versus spatial position. One can offset and expand the spatial variables within the resolution of the PSD in order to maximize the ratio of the signal to noise. The multichannel analyzer has the capability of integrating a marked region of interest. This allows for immediate quantitative comparison of Bragg peaks, along with the qualitative visual display, during an experiment. After the data are acquired, the raw data within the region of interest are stored in a computer for additional off-line detailed analysis.

The precision in the determination of lattice-parameter changes normally obtained in this laboratory was forfeited because of the time requirements imposed by ortho-para conversion. The observed lattice parameters agreed with those in the literature[7] within the sum of the respective estimated experimental uncertainties. In general, the data were not taken with a theta-theta scan but rather with the incident x rays fixed at the Bragg angle.

The most frequent method of observing the transformation was to raise or to lower the temperature while observing the intensity of the fcc Bragg peak. The temperature was stepped in increments ranging from 20 to 100 mK. The sample cell came to thermal equilibrium with a time constant of less than two minutes, in the temperature range of interest. At each temperature Bragg peaks were obtained twice and recorded along with the time and temperature. The Cu$K\alpha$ Bragg peaks were accumulated for 200 sec. The temperature was then changed at a rate of less than 30 mK per minute and the procedure repeated. Because the PSD records all the information necessary to subtract out the background, x-ray filters were not employed. This allowed for an increased intensity and an improvement in signal to noise because of the increased statistics. The above process could be carried out in a time interval of 7 to 15 min. In this manner one could step through both the hcp to fcc and the fcc to hcp transformations as a function of temperature in a narrow concentration range.

Alternatively, the temperature was held constant, and the fcc Bragg peak was observed as a function of time, and hence of decreasing concentration. However, this works only for the fcc to hcp transformation, because the ortho-para conversion cannot be reversed without raising the temperature significantly.

The basic cryogenics consisted of a minidilution refrigerator housed in a set of special Dewars.[17] The Dewar keeps the sample fixed in space relative to the diffractometer during thermal cycling while allowing $\frac{5}{2}\pi$ sr of usable solid angle. There are no cryogenic fluids in the path of the x rays. Cylindrical beryllium and aluminized Mylar windows are used as vacuum and thermal shields.

The cryogenic system was originally designed for use with helium samples with solidification temperatures less than 4 K. For this reason the sample fill-line heaters were not adequate for hydrogen, whose solidification temperature is near 14 K. Rather than completely rebuild the existing fill line, the following modifications were made. Near the sample cell an extra volume was inserted into the fill line. This assured the availability of gas to fill the sample cell with solid, even though the fill line would plug near the helium reservoir. Additional heaters were added to accessible links in the fill line and the extra volume to insure the flow of hydrogen between the extra volume and the sample cell.

It has been found that Lucite sample cells provide a workable combination of physical properties for experiments on helium and hydrogen. Lucite has low thermal conductivity, which is necessary for large single-crystal growth, and is relatively transparent to x rays. The existing Lucite sample cell has an o.d. of 4.0 mm, and i.d. of 1.5 mm, and 12.0 mm of usable length (see Fig. 1). This Lucite cell can withstand pressures up to 10 MPa, which is sufficient for various stages of gas handling and testing. The samples were finally solidified near zero pressure. The upper half of the sample cell was filled with a copper plug coated with Apiezon N grease and press fitted into position. The plug served two purposes. It reduced the sample cell volume by half (heating due to ortho-para conversion is proportional to the number of moles of hydrogen present), and it provided better

thermal contact between the sample and the cold finger. After insertion the remaining volume was thoroughly cleaned and the fill line inserted and secured. The sample cell was then thermally linked from top to bottom. The link was made by wrapping a piece of 0.3-mm diameter copper wire on the outside of the sample cell concentric with the copper plug at the top and the fill-line insert at the bottom. The existing thermal contact of the sample cell to the cold finger of the dilution refrigerator was supplemented with an additional 0.46-mm diameter copper wire wrapped concentric with the above-mentioned copper plug and anchored to a resistance thermometer's mounting screw on the cold finger.

The main thermometry consisted of one carbon and two germanium resistors. One germanium resistor and the carbon resistor were mounted on the cold finger above the sample cell. The second germanium resistor was mounted in the Lucite nut which secured the fill-line seal to the bottom of the sample cell. In addition, a gold-iron versus Constantan differential thermocouple was mounted directly across the sample cell at the thermal link. This was useful in measuring temperature differences across the sample cell at temperatures greater than 1 K and indicated the transfer of hydrogen gas and the onset of solidification.

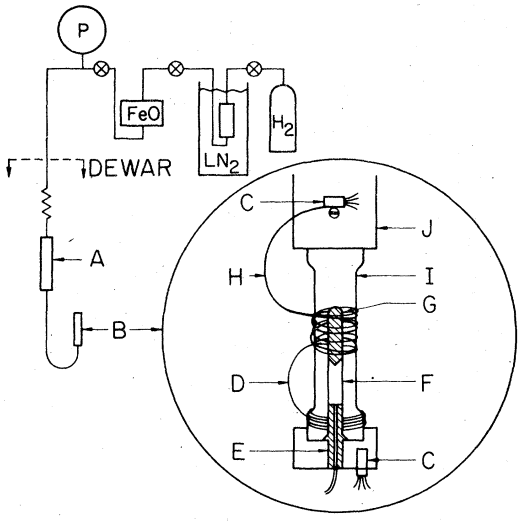

FIG. 1. Gas-handling system. During transfers of He to the Dewar, the fill line would plug above the extra volume (*A*) and the sample cell assembly (*B*). The extra volume contained enough gas to partially fill the crystal-growth region (*F*) with solid hydrogen near zero pressure. A thermal link (*D*) is wrapped concentrically with the copper plug (*G*) and the fill-line entrance (*E*). An additional thermal link (*H*) connects the Lucite sample cell (*I*) to the dilution refrigerator's copper cold finger (*J*). The two germanium thermometers (*C*) are indicated. The differential thermocouple across the crystal growth region and the carbon resistor are not shown.

B. Sample preparation

All samples were extracted from a single bottle of commercially available hydrogen gas of 99.999% purity. Before an experiment the sample cell and gas-handling system were pressurized to 7 MPa and evacuated three times. A simplified schematic of the gas-handling system is shown in Fig. 1. The gas was drawn from the storage cylinder and condensed into a cold trap filled with molecular sieve, Linde type 13*X*, at 77 K. This provided a clean method of moderate pressure generation. The gas was then transferred to an orthohydrogen converter, which consisted of a stainless-steel pressure vessel filled with a catalyst, iron oxide. A starting orthohydrogen concentration of 0.75 was assured by storing the gas in the converter for three days at room temperature.

A typical experiment started with the gas in the converter and the Dewar precooled to a temperature between 40 and 80 K. The cool-down and solidification time in these experiments is significant due to the starting temperature, large heat capacity of the Dewars, and the single-crystal growth. A log of temperature versus time was kept throughout the experiments for the concentration analysis discussed in Sec. III C. At time equal to zero the converter was opened to the sample cell and extra volume. After pressure equilibrium was achieved, typically at 4 MPa in 45 min, the converter was closed off, and liquid helium was transferred to the Dewar. As the Dewar was cooled down, the fill line would plug above the extra volume. However, at this time the extra volume contained enough gas to fill the sample cell partially with solid hydrogen near zero pressure. As the sample cell approached the solidification temperature of hydrogen, appropriate heaters were used to ensure the proper temperatures and temperature gradients for single-crystal growth. The extra volume was held at 20 K, and a temperature difference of less than 0.5 deg was maintained across the sample cell during crystallization. The crystals were grown from the liquid state, progressively from the top to the bottom of the sample cell. The differential thermocouple indicated the onset of crystal growth. The growth time ranged from 5 to 30 min, with no apparent correlation to resulting crystal quality. The completion of crystal growth in the sample cell was dramatically indicated by the thermometers on the extra volume as its hydrogen released its latent heat of solidification.

After modest annealing, one hour, in the hcp structure the sample was cooled into the fcc phase to a temperature near 0.8 K. A series of one- to two-hour transmission Laue pictures was then taken for orientational purposes. Because hydrogen is a poor scatterer of x rays, only the three or four most intense spots were observable in the Laue pictures. Once the {200} fcc Bragg reflection had been identi-

fied and aligned, the crystal could be further inspected for quality and size. Typical dimensions were 1.5 mm in diameter by 2.5 mm in length. Of the ten samples prepared, one was polycrystalline within the x-ray beam diameter, and one was a bicrystal. The angular misorientation in the bicrystal was approximately one degree of arc, and the individual Bragg peaks were resolvable. The other samples consisted of what appeared to be single crystals with dimensions greater than 2 mm in length.

C. Analysis of concentration

Experimental analysis of the orthohydrogen concentration χ at successive stages of measurements on a given specimen, was impractical. The concentration was, therefore, calculated as a function of time from a modified version of the well-established rate equation,[18,19]

$$\frac{d\chi}{dt} = -k\chi^2 \ . \tag{1}$$

Normally one starts at time equal to zero with a concentration of 0.75 and cools to a temperature near 14K in a relatively short time period. However, due to the indicated experimental arrangement in this work the cool-down time ranged from two to seven hours. For this reason the following modified rate equation was used,

$$\frac{d(\chi-\chi_0)}{dt} = -k(\chi-\chi_0)^2 \ , \tag{2}$$

which leads to the solution

$$(\chi-\chi_0)^{-1} = k(t-t_i) + (\chi_i-\chi_0)^{-1} \ , \tag{3}$$

where χ is the concentration at time t, χ_0 is the thermal equilibrium concentration as a function of temperature,[20] χ_i is the initial concentration at the beginning of a time interval starting at time t_i, and k is the rate constant taken to be equal to 0.019 h^{-1}. Equation (3) was first solved using the initial temperature at time equal to zero. It was then solved in variable time intervals, determined by fixed five-degree increments in temperature, as the cooling progressed until the sample reached a temperature of 15 K. For temperatures less than this, χ_0 is essentially zero, and Eq. (2) reverts back to Eq. (1). The effect of this modification for times greater than seven hours, in these experiments, is to displace the concentration versus time curve to higher concentrations.

D. Analysis of the crystallographic transformation

The crystallographic transformation can be observed by crossing the phase boundary as a function of temperature or, alternatively, of concentration (which is implicitly a function of time). Because the physical processes are similar for both variables, the observed results should have similar functional forms. Therefore, the following analysis applies to both methods of taking data with the independent variable being time or temperature. The transformation temperature (time) was defined as the temperature (time) at which the integrated peak intensity, above background, was half the difference between maximum and minimum. This is the same criterion used by Mills and coworkers.[7,8] Alternative analyses of the peak amplitude, of raw integrated intensity (with and without the background subtracted), and of integrated intensities from least-squares curve fitted peaks yielded the same transformation temperatures and times with variations less than the experimental uncertainties.

Define the results of any one of the above methods of analysis as the intensity I as a function of the temperature T. This intensity was fitted to a function of the form,

$$I = A\{1-\tanh[(T-T^*)/B]\} + C \ , \tag{4}$$

where T^* is the transformation temperature (or time), the maximum intensity is given by $2A+C$, the minimum intensity is C, and B characterizes the width of the transformation (see Fig. 2). This form of analysis provides a systematic method of handling the data and parameterizing the transformation width.

III. EXPERIMENTAL RESULTS AND DISCUSSION

A. Crystallographic transformations

The details of the resulting transformation temperatures are summarized in Table I. The six samples listed are from experiments with the sample cell in its final configuration indicated in Fig. 1.

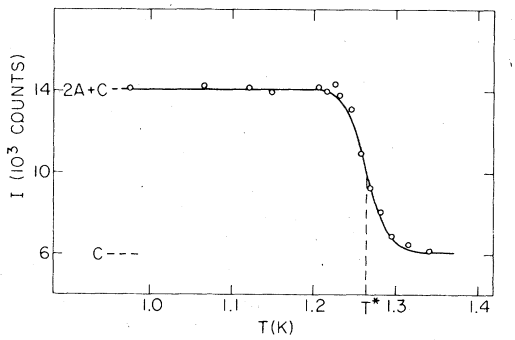

FIG. 2. Bragg peak intensity versus temperature. The integrated intensity of the {200} fcc Bragg peak is plotted as a function of increasing temperature through a fcc to hcp transformation. The solid line is given by Eq. (4) with $T^* = 1.265$ K and $B = 26$ mK. The magnitude of the final intensity C depends upon the angular width chosen for the integration. For this particular transformation, C is approximately 96% background.. See text, Secs. II D and III B.

TABLE I. Summary of transformation characteristics. T^* is the crystallographic transformation temperature. B parameterizes the width of the transformation as defined in Eq. (4). The orthohydrogen concentration x is given in percent. F_B (F_A) represents the fraction of the initial {200} fcc Bragg peak intensity before (after) the transformation.

Run	Method[a]	T^* (K)	B (mK)[b]	x	F_B (F_A)
7	W	1.17	11	64.6	1.0 (0.0)
	C	0.90	37	63.4	0.0 (1.0)
	t	0.17	<7	49.0	1.0 (0.05)
8	W	1.08	21	63.2	1.0 (0.0)
9	W	1.26	26	66.0	1.0 (0.03)
	C	1.00	40	65.3	0.03 (0.87)
	W	1.18	28	63.5	0.87 (0.04)
	C	0.76	122	62.5	0.04 (0.68)
	W	1.10	35	62.1	0.68 (0.07)
	C	0.70	100	61.6	0.07 (0.56)
	t	0.17	6	48.8	0.56 (0.07)
10	W	1.09	48	63.0	1.0 (0.19)
	C	0.66	90	62.1	0.19 (0.68)
	W	0.96	43	61.2	0.68 (0.18)
	C	0.51	140	60.6	0.18[c]
11	W	1.35	16	69.8	1.0 (0.02)
	C	1.21	15	69.2	0.02 (1.0)
	t	1.27	0.26	66.7	1.0 (0.02)
	C	0.96	54	65.5	0.02 (0.90)
	W	0.50	63	52.1	0.90 (0.0)
13	W	1.23	55	65.0	1.0 (0.16)
	C	0.88	79	64.2	0.16 (0.88)
	W	1.06	36	61.0	0.88 (0.19)

[a]Method of crossing the phase boundary between the fcc and hcp crystallographic structures is represented by: W—warming (fcc → hcp), C—cooling (hcp → fcc), t—drift in time (fcc → hcp).
[b]Parameter B is given in units of hours for those transitions crossed as a function of time.
[c]This transformation did not go to completion.

The results of this work are compared with other determinations of the transition temperatures in Fig. 3. The agreement and correlation of previous x-ray results with other experimental studies with T^* greater than 1 K have been discussed in the literature.[8] As can be seen in Fig. 3, the extrapolation (from data taken at higher concentrations) of previous x-ray work[7,8] is in good agreement with the present work's high-concentration data. However, when $x < 0.65$ (for the hcp to fcc transformation) and when $x < 0.55$ (for the fcc to hcp transformation), our results consistently fall below the straight-line extrapolation of Mills.

The striking result of this work is the extension of $T^*_{\text{fcc}\to\text{hcp}}$ and $T^*_{\text{hcp}\to\text{fcc}}$ to temperatures below 0.5 K. The implication of the present data is to exclude the low-concentration NMR results from being associated with a crystallographic transformation. This distinction has also been found at higher pressures[1] and contradicts the belief that the molecular ordering drives the crystallographic transformation.[21]

The interpretation of the present results critically depends upon the coordinates of three data runs, yielding the two points with $T^*_{\text{fcc}\to\text{hcp}}$ equal to 0.17 K and the lower limit in concentration path for the hcp to fcc transformation. The lower limit in concentration for the hcp to fcc transformation (described below) is based not only upon the lack of recovery of the fcc Bragg peak, but also upon the existence of hcp Bragg peaks. The indicated corrections to the transformation temperatures (described below) are straightforward and experimentally supported. Furthermore, the determination of $T^*_{\text{fcc}\to\text{hcp}}$ and the characteristics of the transformation, at high temperatures, were found to be independent of the driving variable, time or temperature, used to cross the phase boundary. There is even a possible advantage in taking a point as a function of time, in that tran-

sient temperature gradients are eliminated. For these reasons the lowest temperature transformation is well established, even though it was crossed only as a function of time. It should be noted that this point was taken on two separate samples with the same results. Furthermore, the temperature at which this point was taken is not the lowest temperature attainable with the dilution refrigerator for the given heat load due to ortho-para conversion. The temperature was chosen to be a point well below the NMR results, but high enough to retain adequate cooling power in the dilution refrigerator so that temperature stability and heat flow were maintained.

In order to investigate possible temperature gradients due to the heating from ortho-para conversion, six separate experiments were performed, with and without: hydrogen, the copper plug, and the thermal links attached to the sample cell. The temperature difference between the cold finger and the bottom of the sample cell was monitored as a function of time and temperature. Warming and cooling data were taken for times up to 150 h (heating due to ortho-para conversion decreases with decreasing ortho concentration). Define ΔT to be the maximum temperature difference between the thermometers on the cold finger and the bulk of the crystal inside the sample cell, assembled in the final configuration. The results of these experiments imply that ΔT is less than 30 mK for all data points except the lowest temperature point, for which ΔT is less than 40 mK. Furthermore, the temperature difference across the length of the sample cell was less than 20 mK. The quoted temperatures in the data presented in this work are the result of adding ΔT to the observed thermometer readings, (i.e., the data have already been compensated for possible temperature differences). This should be a conservative upper limit since the x rays probed the top of the crystal, centered 1 mm from the copper plug, which was in good thermal contact with the cold finger.

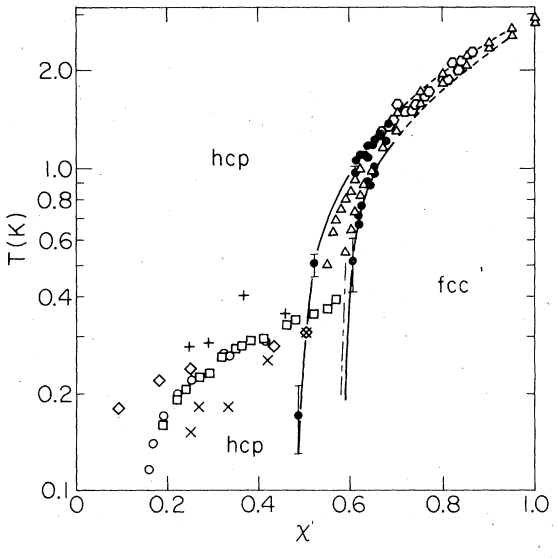

FIG. 3. Transition temperatures versus orthohydrogen concentration. • — x ray, this work; dashed line — x ray, Ref. 7, 8: Δ — $(dP/dT)_V$, Ref. 6; (hex) — NMR (cw), Ref. 3; □ — NMR (cw) Ref. 14; ○ — NMR (cw) Ref. 13b; × — NMR (cw), Ref. 13a; + — NMR (pulsed), Ref. 15; ◇ — NMR (T_1), Ref. 16; short- and long-dash line — lower concentration limit for the hcp to fcc transformation, this work; solid line is to guide the eye only. The upper curve is the fcc to hcp transformation, and the lower curve is the hcp to fcc transformation. Estimated uncertainties in the sample temperatures and temperature gradients have already been accounted for and are indicated (see text, Sec. III A).

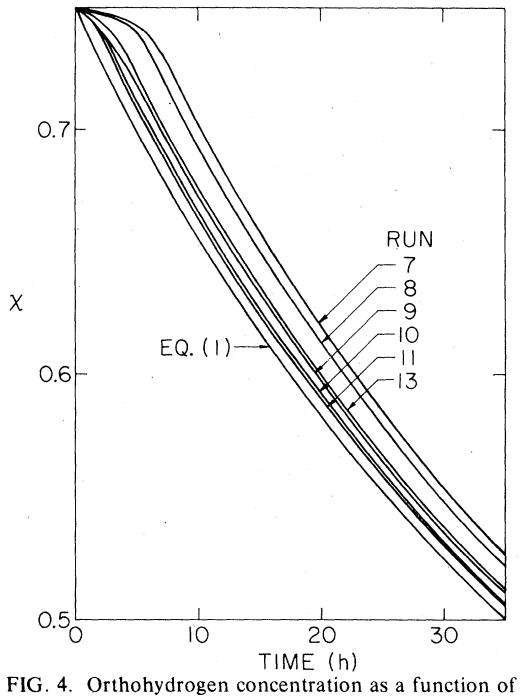

FIG. 4. Orthohydrogen concentration as a function of time. The solutions to Eq. (2), using the appropriate experimental conditions, are compared to Eq. (1).

The reported orthohydrogen concentrations are calculated from Eqs. (1) and (2), based upon the time evolution of the temperature during cooling. The results of these calculations are graphically displayed in Fig. 4. The resulting uncertainty in the determined concentrations is believed to be 0.007. Confidence in the concentration analysis is strengthened by the consistency in the data because each sample was corrected independently. An alternative method would have been to also treat the rate constant k as a function of temperature, and hence of time, as the temperature of the sample was lowered. However, the available information in the literature on the temperature dependence of k, for temperatures greater than 20 K, is limited and not consistent. Therefore, this refinement has been ignored.

The estimated uncertainties for T^* in Fig. 3 are $\pm \Delta T$ discussed above, with one exception. The exception is the hcp to fcc transformation at 0.51 K. The estimated uncertainties for this point (see Figs. 3 and 5) are the result of the following experimental problem. There was an inherent timing difficulty in cooling through a transformation whose temperature lies between 0.5 and 0.7 K. The width of the transformations would dictate that one observe the Bragg intensity over a temperature range of at least 300 mK. The difficulty lies in starting the refrigerator as a true dilution refrigerator, which happens near 0.6 K. During one of these experiments the dilution refrigerator may be started and stopped three or four times in cycling through the transformation temperatures. In practice, the first time it is started it is usually smooth and responsive to known experimental perturbations. However, after warming above 0.7 K for extended time periods, the liquid interfaces in the dilution refrigerator may prevent proper operation. The time required to rectify the interface levels may be from one to ten hours. During this time the orthohydrogen concentration has significantly changed. At concentrations near 0.6, the slope of the phase boundary for the hcp to fcc transformation is steep enough to prevent one from reentering the fcc phase if there is too long a time delay. However, if the sample partially transforms back into the fcc phase, the present method of analysis allows one to extract the transformation temperature with somewhat larger error bars. This is what happened to the point at 0.51 K.

The time delay in starting the dilution refrigerator occured in several samples during an attempt to reenter the fcc phase below 0.6 K. However, once the dilution refrigerator was started, there was no problem in cooling to 0.2 K. As a result, one can at least place a lower concentration limit on the hcp to fcc transformation if the sample does not reenter the fcc phase. The unevenly dashed curve in Fig. 3 is such a concentration-temperature path. It represents the highest observed concentration for which the sample failed to reenter the fcc phase and is considered to be a lower limit for this transformation.

The parameterization of the widths of the transformation is described in Sec. II D above. Approximately 76% of the transformation has taken place in the temperature interval $2B$ and 95% in $3.68B$. For those points taken by drifting in time, the parameter B has the units of time. These widths in time have been converted to temperature, and are included in Fig. 5, by using the local time derivatives of the concentration and the apparent concentration derivative of the transformation temperature. The large error bar for the point with T^*, equal to 0.17 K in Fig. 5, is the result of the uncertainty in the concentration derivative of the transformation temperature. The warming, cooling, and drift in time experiments were equally well fit by Eq. (4). All the transformations appeared as smooth variations in the Bragg intensity with a systematic increase in the transformation width as the transformation temperature was lowered. As can be seen in Fig. 5, within the scatter of the data, there is no obvious distinction in the width of the transformation as a function of experimental method: warming, cooling, or drift in time.

B. Additional experimental observations

In this section we discuss several general characteristics of the Bragg peaks worth mentioning, but which may not have conclusive implications. The beam divergence and the detector resolution were on the order of 6 min of arc each, while the typical full width at half-maximum of the Bragg peak was about 30 min of arc. This is considerably larger than the other quantum crystals[22] and noble-gas crystals[23] studied in this laboratory and is partially due to the limited growth and annealing time. It is plausible that peak broadening was dominated by stacking faults, although analysis such as that carried out by Yarnell and coworkers[11] on polycrystalline deuterium was not possible with our single crystals.

Computer analyses of the recorded data allowed the center of the Bragg peak to be found reproducibly to within 1 min of arc, the reproducibility being sta-

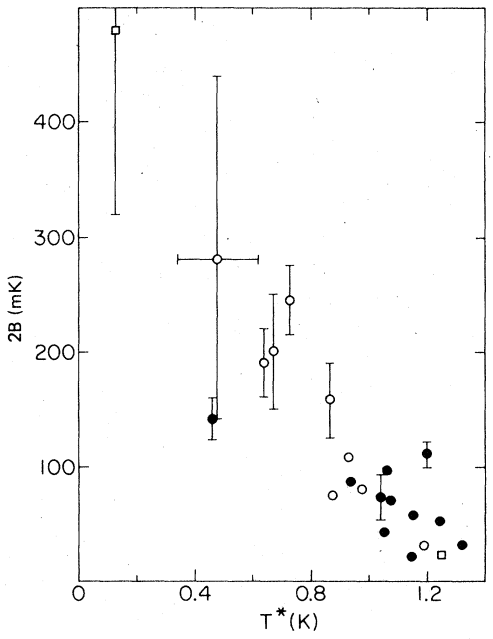

FIG. 5. Widths of the observed transformations. The parameter $2B$, resulting from the analysis of the data using Eq. (4), is plotted vs the transformation temperature. The methods of producing the transformation are represented by: • — warming (fcc → hcp), ○ — cooling (hcp → fcc), □ — drift in time (concentration — fcc → hcp).

tistically limited by the number of counts. As commented upon by Schuch,[8] the peak centers were stationary within this statistical limit over wide temperature ranges in both the hcp and fcc phases. Furthermore, the fcc peak reappeared in the same position, within 1 min of arc, after excursions into the hcp phase.

The basic characteristics of the transformations at higher concentrations have been reported by Schuch and Yarnell with emphasis on deuterium. In general, the same comments apply to the hydrogen studies of the present work with the exception of the stability of the fcc phase with cycling through the transformation. Unlike the results of Schuch for hydrogen and deuterium, here it was found that the {200} Bragg reflection did not always return to its original intensity after a transformation into the hcp phase and back. The percent decrease of the intensity with each transformation ranged from 0 to 32% and is indicated in Table I. However, like previous results for deuterium[8,11] and hydrogen,[8] in some samples there existed a small fraction of the fcc phase well into the hcp structure. This residue fcc structure in the hcp phase appeared to be thermally and not concentration activated, i.e., the intensity seemed to be independent of time but rather disappeared as the temperature was raised.

On several occasions this residue fcc Bragg peak was monitored as a function of temperature for $\chi < 0.5$ near the low-concentration NMR transitions. There is no reason to expect the x-ray results to reveal the orientational ordering transition unless the residue fcc phase is stabilized by the ordered molecules. If this were true, one might expect a more rapid decrease in the residue fcc peak for temperatures above the observed NMR transition. One such residue fcc {200} Bragg peak was monitored for $0.15 < T < 0.6$ K at $\chi = 0.53$. There was a 4% decrease in the integrated intensity centered at $T = 0.38$K over a 200-mK region, while the noise level was approximately 1%. In a second sample, a similar residue fcc peak faded linearly with temperature for $T < 0.14$ K and $\chi = 0.42$. A third sample's residue fcc peak disappeared linearly with temperature for $0.17 < T < 0.40$ K with $0.44 > \chi > 0.40$, held relatively constant for $0.40 > \chi > 0.33$ with $T = 0.40$ K and continued to decrease with increasing temperature for $T > 0.40$ K.

In all the direct observations of the transformation temperatures, only the fcc phase was monitored. However, once the sample failed to reenter the fcc phase, the hcp structure was examined and the $\{10\bar{1}1\}$ and $\{10\bar{1}0\}$ Bragg peaks were monitored, specifically for observing the melting of the crystal. In addition to the residue fcc peaks in two samples, the $\{10\bar{1}1\}$ hcp Bragg reflections were monitored as a function of temperature near the NMR transitions. For the first sample the intensity was constant in the temperature range $0.1 < T < 0.43$ with $\chi = 0.3$. Direct comparison for higher temperatures is not available. For the second sample the intensity varied less than 10% in the temperature range $0.1 < T < 11.0$ K with $0.23 < \chi < 0.25$. There was no systematic variation in the Bragg intensity near the NMR transitions. The small increase in the hcp intensity at higher temperatures is contrasted with the large recovery of the hcp phase in the samples of Schuch.

No attempt was made to verify the volume change at the transformation by directly observing the lattice parameters on both sides of a transformation. But similarly to Schuch, on one occasion the fcc {111} Bragg peak was observed through the fcc to hcp transformation at $\chi = 0.55$ over the temperature range $0.2 < T < 0.92$ K. This peak transformed into the hcp {0002} reflection with no apparent change in intensity or Bragg angle. This is consistent with, but does not verify, the volume change of 0.08% (on warming) reported by Jarvis and co-workers.[5] The lack of confirmation stems from the relative insensitivity of these experiments to changes in lattice parameters. If one assumes an ideal $\hat{c}$ to $\hat{a}$ ratio (accurate to 1 part in 1200)[11] in the hcp phase, the implied volume change would be zero. However, the experimental limit on the $\hat{c}$ to $\hat{a}$ ratio would allow for a 0.1% volume change in going from the fcc to hcp phase (consistent with the 0.08% value). The magnitude of this volume change would alter the Bragg angle, in going from the fcc {111} to the hcp {0002}, by approximately 7 sec of arc. This is compared to the 1 min of arc sensitivity employed in these experiments and is consistent with no observed change.

IV. CONCLUSION

The x-ray diffraction techniques of this work have mapped the fcc to hcp and hcp to fcc phase transformations in solid hydrogen near zero pressure for temperatures below 1.5 K. The fcc to hcp transformation extrapolates to zero temperature near a concentration of 0.49, while the lower concentration limit for the hcp to fcc transformation extrapolates to zero temperature near a concentration of 0.58. The present observations of a crystal-structure change in hydrogen, which do not coincide with the low-concentration NMR results, support two findings from analysis of the NMR line shapes in the limit as T tends to zero as a function of concentration. First, it had been found[24] that the zero-point motion correction factor to the splitting in the peak derivative line shape was slightly different, 10%, for $\chi < 0.5$ and for $\chi > 0.5$. Theoretical calculations[10,21,25,26] of quantum-mechanical energies suggest some difference due to the difference in the structural symmetries. Second, it appears[14] that the long-range molecular rotational order, space group $Pa3$, found for $\chi > 0.5$ is lost for $\chi < 0.5$. It has been suggested

that the low-concentration ordered state is a quadrupole spin-glass.[14] However, theoretical predictions of long-range ordered hcp phases also exist in the literature.[21,25]

Observations of (a) broadened Bragg peaks, and (b) the temperature region over which the transformations occur which increases with decreasing T^*, generally agree with those in the literature at higher temperatures. Observations made in an attempt to determine whether the rotationally ordered molecules stabilized the residue fcc phase in the predominantly hcp structure are inconclusive. However, the results of this work and of other work at elevated pressures[1] indicate that the molecular ordering is not the dominant competing factor which drives the crystallographic transformation in the bulk of the specimen.

ACKNOWLEDGMENTS

We acknowledge stimulating conversations with A. J. Berlinsky, W. Biem, J. H. Constable, W. N. Hardy, A. B. Harris, H. Meyer, J. C. Raich, I. F. Silvera, N. S. Sullivan, and H. Vinegar. This work was supported in part by the U.S. DOE under Contract No. EY-76-C-02-1198.

---

*Present Address: Measurex Corp., Cupertino, Calif. 95014.

[1]R. L. Mills, J. Low Temp. Phys. 31, 423 (1978), and references contained therein.
[2]F. Reif and E. M. Purcell, Phys. Rev. 91, 631 (1953).
[3]G. W. Smith and R. M. Housley, Phys. Rev. 117, 732 (1960).
[4]G. Ahlers and W. H. Orttung, Phys. Rev. 133, A1642 (1964).
[5]J. Jarvis, D. Ramm, and H. Meyer, Phys. Rev. Lett. 18, 119 (1967).
[6]J. Jarvis, H. Meyer, and D. Ramm, Phys. Rev. 178, 1461 (1969).
[7]R. L. Mills, A. F. Schuch, and D. A. Depatie, Phys. Rev. Lett. 17, 1131 (1966).
[8]A. F. Schuch, R. L. Mills, and D. A. Depatie, Phys. Rev. 165, 1032 (1968).
[9]H. M. James and J. C. Raich, Phys. Rev. 162, 649 (1967).
[10]H. Miyagi and T. Nakamura, Prog. Theor. Phys. 37, 641 (1967).
[11]J. L. Yarnell, R. L. Mills, and A. F. Schuch, Sov. J. Low Temp. Phys. 1, 366 (1975).
[12]W. N. Hardy, I. F. Silvera, and J. P. McTaguee, Phys. Rev. B 12, 753 (1975).
[13]N. S. Sullivan, H. Vinegar and R. W. Pound, Phys. Rev. B 12, 2596 (1975); H. J. Vinegar, J. J. Byleckie, and R. W. Pound, Phys. Rev. B 16, 3016 (1977).
[14]N. S. Sullivan, M. Devoret, B. P. Cowan, and C. Urbina (unpublished).
[15]D. L. Husa and J. G. Daunt (unpublished).
[16]H. Ishimoto, K. Nagamine, and Y. Kimura, J. Phys. Soc. Jpn. 35, 300 (1973).
[17]S. M. Heald and R. O. Simmons, Rev. Sci. Instrum. 48, 56 (1977).
[18]F. Schmidt, Phys. Rev. B 10, 4480 (1974), and references contained therein.
[19]K. Motizuki and T. Nagamiya, J. Phys. Soc. Jpn. 11, 93 (1956).
[20]L. Farkas, in *Ergebnisse der Exakten Naturwissenschaften* (Springer, Berlin, 1933), Vol. 12, p. 171.
[21]R. J. Lee and J. C. Raich, Phys. Rev. B 5, 1591 (1972) and references contained therein.
[22]B. A. Fraass, S. M. Heald, and R. O. Simmons, J. Cryst. Growth 42, 370 (1977).
[23]D. N. Batchelder, D. L. Losee, and R. O. Simmons, in *Crystal Growth,* edited by H. S. Peiser (Pergamon, New York, 1967), p. 843.
[24]P. L. Pedroni, R. Schweizer, and H. Meyer, Phys. Rev. B 14, 896 (1976), and references contained therein.
[25]H. M. James, Phys. Rev. 167, 862 (1968).
[26]C. Feldman, Proc. Phys. Soc. London 86, 865 (1965).